Am J Nucl Med Mol Imaging 2014;4(4):311-323
www.ajnmmi.us /ISSN:2160-8407/ajnmmi0000157

Original Article

Preclinical evaluation of ^{111}In-DTPA-INCA-X anti-Ku70/Ku80 monoclonal antibody in prostate cancer

Susan Evans-Axelsson[1], Oskar Vilhelmsson Timmermand[2], Charlotte Welinder[3], Carl AK Borrebaeck[4], Sven-Erik Strand[2,5], Thuy A Tran[5], Bo Jansson[3*], Anders Bjartell[1*]

[1]Division of Urological Cancers, Department of Clinical Sciences Malmö, Lund University, Sweden; [2]Department of Medical Radiation Physics, Clinical Sciences, Lund University, Lund, Sweden; [3]Department of Oncology, Clinical Sciences, Lund University, Lund, Sweden; [4]Department of Immunotechnology and CREATE Health Translational Cancer Center, Lund University, Medicon Village, Lund, Sweden; [5]Lund University Bioimaging Center, Lund, Sweden. [*]Equal contributors.

Received March 5, 2014; Accepted May 14, 2014; Epub June 7, 2014; Published June 15, 2014

Abstract: The aim of this investigation was to assess the Ku70/Ku80 complex as a potential target for antibody imaging of prostate cancer. We evaluated the *in vivo* and *ex vivo* tumor targeting and biodistribution of the ^{111}In-labeled human internalizing antibody, INCA-X (^{111}In-DTPA-INCA-X antibody), in NMRI-nude mice bearing human PC-3, PC-3M-Lu2 or DU145 xenografts. DTPA-conjugated, non-labeled antibody was pre-administered at different time-points followed by a single intravenous injection of ^{111}In-DTPA-INCA-X. At 48, 72 and 96 h post-injection, tissues were harvested, and the antibody distribution was determined by measuring radioactivity. Preclinical SPECT/CT imaging of mice with and without the predose was performed at 48 hours post-injection of labeled DTPA-INCA-X. Biodistribution of the labeled antibody showed enriched activity in tumor, spleen and liver. Animals pre-administered with DTPA-INCA-X showed increased tumor uptake and blood content of ^{111}In-DTPA-INCA-X with reduced splenic and liver uptake. The *in vitro* and *in vivo* data presented show that the ^{111}In-labeled INCA-X antibody is internalized into prostate cancer cells and by pre-administering non-labeled DTPA-INCA-X, we were able to significantly reduce the off target binding and increase the ^{111}In-DTPA-INCA-X mAb uptake in PC-3, PC-3M-Lu2 and DU145 xenografts. The results are encouraging and identifying the Ku70/Ku80 antigen as a target is worth further investigation for functional imaging of prostate cancer.

Keywords: Ku80/Ku80, INCA-X monoclonal antibody, prostate cancer, tumor targeting, preclinical SPECT/CT

Introduction

Radiolabeled monoclonal antibodies directed to cell-surface antigens specifically expressed by cancer cells have shown a potential for cancer imaging and therapy. Unfortunately, this has not yet been successfully developed and implemented in several malignancies. Prostate cancer is a variable and multifocal disease with a variety of potential tumor-associated imaging biomarkers [1-3]. Yet, the only clinically approved radiolabeled antibody for prostate cancer imaging is ProstaScint®, a murine ^{111}In-labeled anti-prostate specific membrane antigen (PSMA) antibody that does not bind other prostate-specific antigens like prostatic acid phosphatase (PAP) or prostate-specific antigen (PSA) [4]. A downfall of ProstaScint® is that the antibody binds to the internal domain of PSMA making image interpretation difficult. It is also hindered by high accumulation in necrotic areas and uptake in normal tissues like the gut, liver and kidneys [5]. This illustrates the obvious need for new validated prostate tumor biomarkers to create a basis for *in vivo* imaging and therapies. Accordingly, there are many antibodies and antibody based conjugates in early stages of clinical development aimed at the selective delivery of therapeutic agents to prostate cancer (http://clinicaltrials.gov NLM Identifiers: NCT00031187, NCT00859781, NCT00054574, NCT01414283, NCT01414296, NCT01631552).

The INCA-X antibody used in this study was selected from a large human antibody library [6] and a pool of cancer cell lines using phage display technique and rapid internalization as a selection criteria [7]. INCA-X has been demonstrated to be specific for cell surface exposed epitopes associated with the Ku70/Ku80 complex. The Ku-antigens are part of a protein complex involving at least two proteins, Ku70 (XRCC6) and Ku80 (XRCC5) [8, 9], originally defined as a nuclear auto-antigen [8]. The first described function was its role in DNA double strand break (DSB) repair through non-homologous end-joining (NHEJ) [10, 11]. Interestingly, Ku-deficient mice and men with prostate cancer who undergo castration therapy are hypersensitive to ionizing radiation [12]. This is likely due to decreased levels of the Ku70 protein in prostate cancer cells after castration therapy [13]. In addition to the DNA repair mechanism, the Ku proteins take part in many different processes. Such cellular processes include: V(D)J recombination [14], telomere maintenance [15-17], transcription regulation [18, 19], integrin function [20], a possible receptor for DNA [21], an androgen receptor recycle co-activator [19] and a carrier of proteolytic enzymes [20]. At present, the function and molecular mechanisms behind the Ku complex is not fully understood, though it is known to have pro-survival and pro-invasive roles essential for tumor progression.

The Ku70/Ku80 antigen is expressed in the nucleus of all cells. However, several studies have revealed that under certain conditions, and in various tumor cell lines, including: glioma cells, neuroblastoma cells, breast and prostate cancer cell lines, the Ku70/Ku80 antigen relocates to the plasma membrane where it is thought to play a role in invasion, migration and cell adhesion [7, 20, 22-25]. The essential multifunction of the protein complex and its surface expression makes it a suitable target for imaging prostate cancer cells. Moreover, the available surface expression of Ku70/Ku80 complex on tumor cells could be harnessed as a possible marker of patient radiosensitivity after castration therapy and before curative radiotherapy begins. In addition to that, the Ku70/Ku80 tumor-associated antigen could provide a receptor-mediated gateway for the potential to deliver antibody-drug conjugates or radionuclides directly to the prostate cancer cells, potentially reducing the systemic toxicity associated with conventional treatments [7, 26].

INCA-X has been shown to rapidly internalize via endocytosis into a variety of tumor cell lines *in vitro* and also showed a strong immunotoxic effect on human prostate cancer PC-3 cells (92% inhibition) when conjugated to Saporin [7, 23]. Considering the previous *in vitro* findings, we went further to investigate the *in vivo* tumor-targeting potential and whole-body biodistribution of radiolabeled INCA-X in nude mice bearing subcutaneous xenografts of human prostate cancer cell lines. For this investigation we used a preclinical small animal dual modality single-photon emission computer tomography/computer tomography (SPECT/CT) imaging system alongside traditional *ex vivo* biodistribution studies.

Materials and methods

Cell lines and cell culture

The androgen independent human prostate cancer cell lines PC-3 (derived from a human bone metastasis), PC-3M-Lu2 (a metastatic clone of PC-3 cells stably transfected with firefly luciferase gene (luc2)) and DU145 (derived from a human brain metastasis) were chosen for this study since they all express the Ku70 and Ku80 antigens [27]. The PC-3 and DU145 cell lines were purchased from ATCC (Manassas, VA) and cultured as a monolayer in HAM's F12 (PC-3) or RPMI (DU145) medium and supplemented with 10% FBS and 1% penicillin-streptomycin (PEST). PC-3M-Lu2 cells (Caliper, Hopkinton, MA) were cultured as a monolayer in EMEM medium, supplemented with 10% heat inactivated FBS and 1% PEST. All cells were kept at 37°C in an atmosphere of 5% CO_2. Cells were regularly tested for mycoplasma and found free of mycoplasma prior to inoculations.

Prostate tumor model

Male athymic NMRI-nude mice (Taconic Europe, Denmark) aged between six and eight weeks old and with a mean body weight of 37 g (range: 31.5-42 g) were used for this study. The animals were provided autoclaved food and water *ad libitum* and housed in individually ventilated cages under sterile conditions; maximum of five mice per cage. The tumor model was obtained by subcutaneous injection of PC-3,

PC-3M-Lu2 or DU145 cells into the lower right flank (3-5 × 10^6 cells in 200 µL medium).

Conjugation and ^{111}In-labeling

Conjugation with chelator: The INCA-X human monoclonal IgG_1 lambda antibody [6, 28] was supplied by BioInvent (Lund, Sweden). The protein solution (5 mg/mL in PBS) was conjugated with the chelator CHX-A"-DTPA (Macrocyclics, USA) in 0.07 M sodium borate buffer, pH 9.2, using a molar ratio of 3:1 chelator to antibody at 40°C. The reaction was terminated after four hours and CHX-A"-DTPA-INCA-X, from now referred to as DTPA-INCA-X, was separated from free chelate by size-exclusion chromatography on a NAP-5 column (GE Healthcare) equilibrated with 20 mL 0.2 M ammonium acetate buffer, pH 5.5. Conjugated INCA-X was eluted with 1 mL ammonium acetate buffer and aliquoted samples were stored at -20°C.

Radiolabeling of DTPA-INCA-X

DTPA-INCA-X in ammonium acetate buffer (50 µl, ~1 mg/mL), pH 5.5, was mixed with a predetermined amount of $^{111}InCl_3$ (~50 MBq, Mallindkrodt, The Netherlands). After incubation at room temperature for one hour, the labeling was terminated and equilibrated with PBS. Labeling efficiency was monitored with ITLC strips (Biodex, USA) and eluted with 0.2 M citric acid. In this system, the radiolabeled conjugate remains at the origin line, while free indium migrates with the front of the solvent. The radioactivity distribution was determined with a PhosphorImager system (Perkin Elmer, Wellesley, MA, USA) using the Optiquant as quantification software (Perkin Elmer).

The labeling yield of ^{111}In-DTPA-INCA-X was greater than 95% as determined by thin layer chromatography and required no further purification.

Flow cytometry

The antibody binding, Ku70 and Ku80 cell surface expression were analyzed by flow cytometry (FACS). PC-3 cells were incubated for one hour with individual antibodies at a concentration of 10 µg/mL in PBS containing 0.5% w/v bovine serum albumin. Primary antibodies were INCA-X (human IgG_1, lambda), anti-Ku70 (mouse IgG, clone N3H10, Abcam, Cambridge, UK), and anti-Ku80 (mouse IgG, clone 111, Abcam). Bound antibody was detected with anti-human Ig APC or anti mouse Ig APC (Jackson Immuno Research, USA). Dead cells were excluded by SYTOX Green Nucleic Acid Stain (Molecular Probes). All incubations were performed on ice. Cells were analyzed with a FACSCalibur (BD Bioscience, California, USA).

Binding specificity of ^{111}In-DTPA-INCA-X

PC-3 cells were cultivated in a Petri dish with a diameter of 3.5 cm to a cell density of 2-5 × 10^5 cells per dish. Labeled conjugates (4 µg/dish) were added to two groups of Petri dishes containing PC-3 cells. A 100-fold excess of non-radiolabeled (cold) INCA-X was pre-administered to one group of dishes 30 minutes before the labeled conjugate was added. The cells were incubated for two hours at 37°C and incubation media was collected. The cells were washed three times with cold serum-free medium and treated with 0.5 mL trypsin-EDTA solution (0.25% trypsin, 0.02% EDTA in PBS buffer) for 10 minutes at 37°C. When the cells were detached, 0.5 mL complete medium was added to every dish and the cells were re-suspended. The cell suspension was collected for radioactivity measurements. Cell-associated radioactivity (C) was measured with an automated gamma counter (1480 Wizard OY; Wallac) in parallel with 1 mL corresponding incubation medium (M). The percentage (%) of added radioactivity bound to cells was calculated as = $C \times 100\%/(C+M)$.

Internalization and retention of ^{111}In-DTPA-INCA-X

The internalization rate of the labeled conjugate was determined on PC-3 cells. Shortly, PC-3 cells were seeded in 6 well plates at 5 × 10^5 cells/well one day prior to the experiment. The cells were incubated for three hours at 4°C on ice with 4 µg/dish of ^{111}In-labeled INCA-X. Thereafter, the incubation medium was discarded and the cells were washed three times using ice-cold serum-free medium. After the addition of 1 mL medium, the cells were further incubated at 37°C. At designated time points, up to three days, one group of three dishes was analyzed for cell-associated radioactivity. Medium was collected, cells were washed three times with ice-cold serum-free medium (these two steps were omitted for the time-point 0 hour) and treated with 0.5 mL of 4 M urea solu-

tion containing 0.2 M glycine buffer, pH 2.5, for five minutes on ice. The acid fraction was collected and the cells were washed with an additional 0.5 mL acid solution. The radioactivity in the acid wash fraction was considered membrane-bound radioactivity. After the addition of 0.5 mL of 1 M NaOH, the cells were incubated at 37°C for 30 minutes and the basic solution was collected. The cell dishes were washed with an additional 0.5 mL of basic solution. The radioactivity in the alkaline fractions was considered internalized radioactivity. The radioactivity content of the samples was measured as mentioned above.

Whole-body in vivo imaging studies

SPECT imaging was carried out on a preclinical dual-modality SPECT/CT system (Nano SPECT/CT plus, Bioscan Inc., Washington, DC) equipped with four gamma cameras and multi pinhole apertures (NSP-106 mouse collimator) with each pinhole measuring 1 mm in diameter. Two NMRI-nude mice bearing PC-3M-Lu2 subcutaneous tumors were designated as either predose group 1 or non-predose group. Five NMRI-nude mice bearing DU145 subcutaneous tumors were designated as: predose group 1, predose group 2, predose group 3, or the non-predose group. Under isofluorane anesthesia, PC-3M-Lu2 and DU145 tumor-bearing mice in predose group 1 were pre-administered intravenously approximately 330 μg of DTPA-conjugated, non-labeled INCA-X 24 hours before the second tail vein injection of ^{111}In-DTPA-INCA-X (10-15 MBq [270-405 μCi], 20 μg INCA-X). DU145 tumor-bearing mice in group 2 and group 3 were pre-administered non-labeled DTPA-INCA-X (330 μg) at 48 hours before (group 2) or immediately before (group 3) the second tail vein injection of ^{111}In-DTPA-INCA-X (same amount as group 1). The non-predose group was given a single tail vein injection of ^{111}In-DTPA-INCA-X only (10-15 MBq [270-405 μCi], 20 μg INCA-X). All mice imaged via preclinical SPECT/CT were sacrificed by isofluorane overdose 48 hours post-injection of ^{111}In-DTPA-INCA-X and imaged post-mortem in the prone position. For anatomic co-registration, CT imaging of the animals was preformed with the combined scanner prior to each SPECT scan and without movement of the animal. Both imaging modalities were registered by hardware calibration. Reconstruction of the SPECT data was performed using HiSPECT software (SciVis Goettingen, Germany). InVivoScope 2.00patch4 software was used for visualization analysis of the SPECT images.

Ex vivo biodistribution studies

Biodistribution studies were performed with and without a pre-administered dose of cold DTPA-conjugated antibody in male NMRI-nude mice bearing human DU145 (n = 7) or PC-3 (n = 15) subcutaneous xenografts. The mice were divided into groups of three to four mice per group and the studies began when the tumors reached a volume larger than 50 mm^3. Under isofluorane anesthesia, mice grouped to receive a pre-administered dose of cold antibody were given an intravenous injection of DTPA-INCA-X (1-1.6 mg) 24 hours prior to the tail vein injection of ^{111}In-DTPA-INCA-X (0.3-0.4 MBq [8-11 μCi], 15 μg of INCA-X). The other group of mice received a single tail vein injection of ^{111}In-DTPA-INCA-X (0.3-0.4 MBq [8-11 μCi], 15 μg of INCA-X). The predosed and non-predosed DU145 tumor-bearing mice were sacrificed at 48 hours post-injection. The PC-3 tumor-bearing mice were sacrificed at 48 hours (including all predosed mice), 72 hours and 96 hours post-injection. Selected organs, blood and tumor were collected and placed in pre-weighed plastic vials. The labeled antibody distribution was determined by measuring radioactivity using an automated gamma counter along with known standards. The tissue and tumor uptake was decay-corrected and calculated as the mean percentage of injected activity per gram of tissue (%IA/g), tumor-to-organ (T/O) and organ-to-blood (O/Bl) ratios and as the standard deviation (SD) of the mean values.

Ethic statement

All animal studies were approved and performed in strict accordance with the guidelines set by the Malmö-Lund Ethical Committee, Lund University for the use and care of laboratory animals (Permit Number: M40-11). All efforts were made to strictly minimize animal suffering.

Results

Ku70/Ku80 expression in vitro

INCA-X has been shown to bind to and internalize into PC-3 human prostate cancer cells *in*

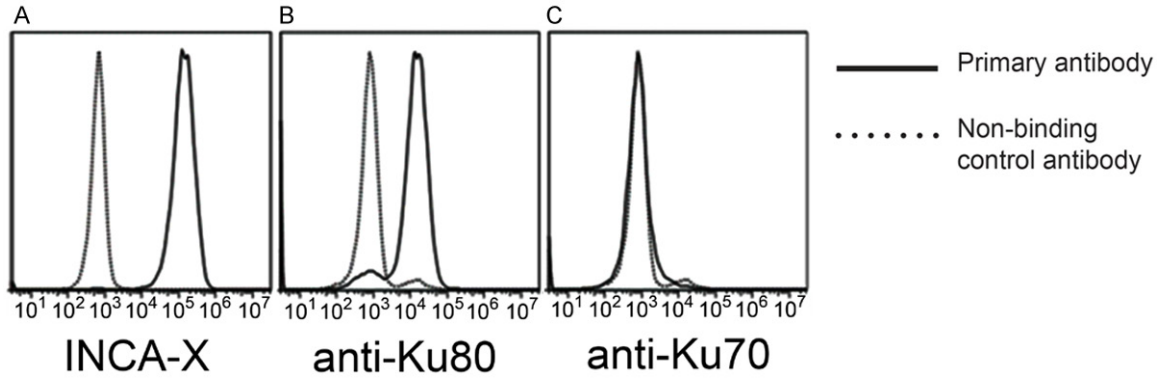

Figure 1. Flow cytometry of PC-3 cells. (A) INCA-X. (B) Anti-Ku80 and (C) anti-Ku70. Dotted lines represent non-binding isotype control antibody and solid lines represent the primary antibody.

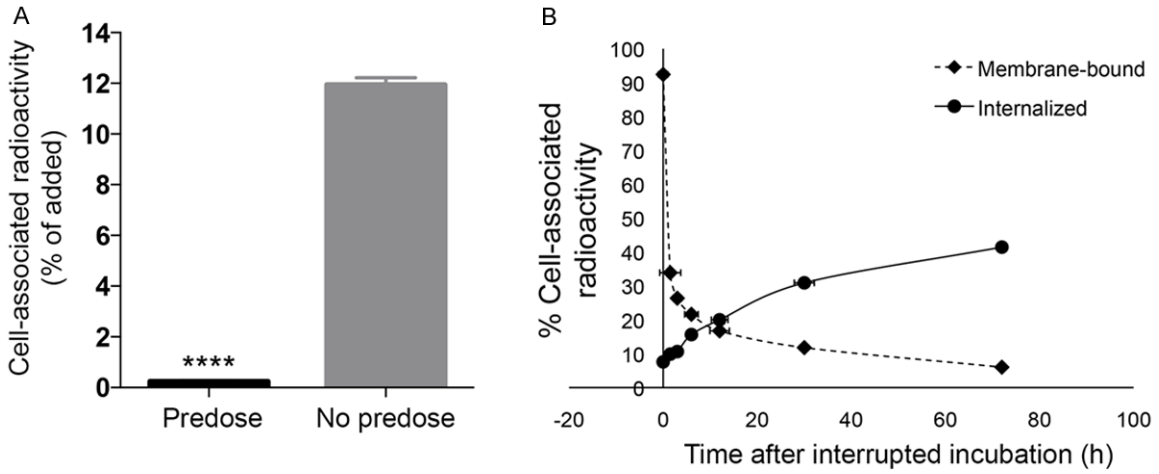

Figure 2. *In vivo* binding specificity and internalization of ^{111}In-DTPA-INCA-X on PC-3 cells. (A) Blocking assay showing the binding specificity of ^{111}In-DTPA-INCA-X to PC-3 cells. (B) Cellular retention and internalization of ^{111}In-DTPA-INCA-X on PC-3 cells. Error bars represent mean ± standard error. ****: P<0.0001.

Table 1. Biodistribution (%IA/g) of ^{111}In-DTPA-INCA-X in nude mice bearing PC-3 tumors

	^{111}In-INCA-X			
	48 h (predose, n = 3)	48 h (n = 4)	72 h (n = 4)	96 h (n = 4)
Tumor	13.09 ± 1.04	7.51 ± 3.07	12.08 ± 16.35	14.81 ± 9.48
Blood	21.38 ± 1.33	4.66 ± 1.74	1.99 ± 1.99	0.49 ± 0.47
Spleen	12.06 ± 1.55	101 ± 17.80	129 ± 33.73	174 ± 23.46
Lungs	12.98 ± 5.86	7.79 ± 1.50	3.77 ± 2.13	1.82 ± 0.20
Kidneys	10.39 ± 0.65	9.40 ± 2.90	5.59 ± 1.20	4.13 ± 0.98
Liver	8.42 ± 0.29	18.37 ± 10.80	14.98 ± 3.37	16.22 ± 2.90
Muscle	3.26 ± 1.25	0.73 ± 0.25	0.54 ± 0.16	0.66 ± 0.36

vitro [7]. We confirmed the binding results by FACS, illustrating INCA-X binding to the surface of PC-3 cells (**Figure 1A**). The anti-Ku70 binding on the surface of PC-3 cells (**Figure 1C**) was weak compared to that of the anti-Ku80 binding (**Figure 1B**) when assayed via FACS.

To investigate the *in vitro* targeting capabilities of radiolabeled INCA-X, blocking assays were performed on the PC-3 prostate cancer cell line. From these tests, we show that the binding of ^{111}In-DTPA-INCA-X to PC-3 cells was specific since the uptake of ^{111}In-DTPA-INCA-X was significantly blocked by the excess of cold INCA-X (P<0.0001) (**Figure 2A**). The cellular processing of ^{111}In-DTPA-INCA-X is illustrated in

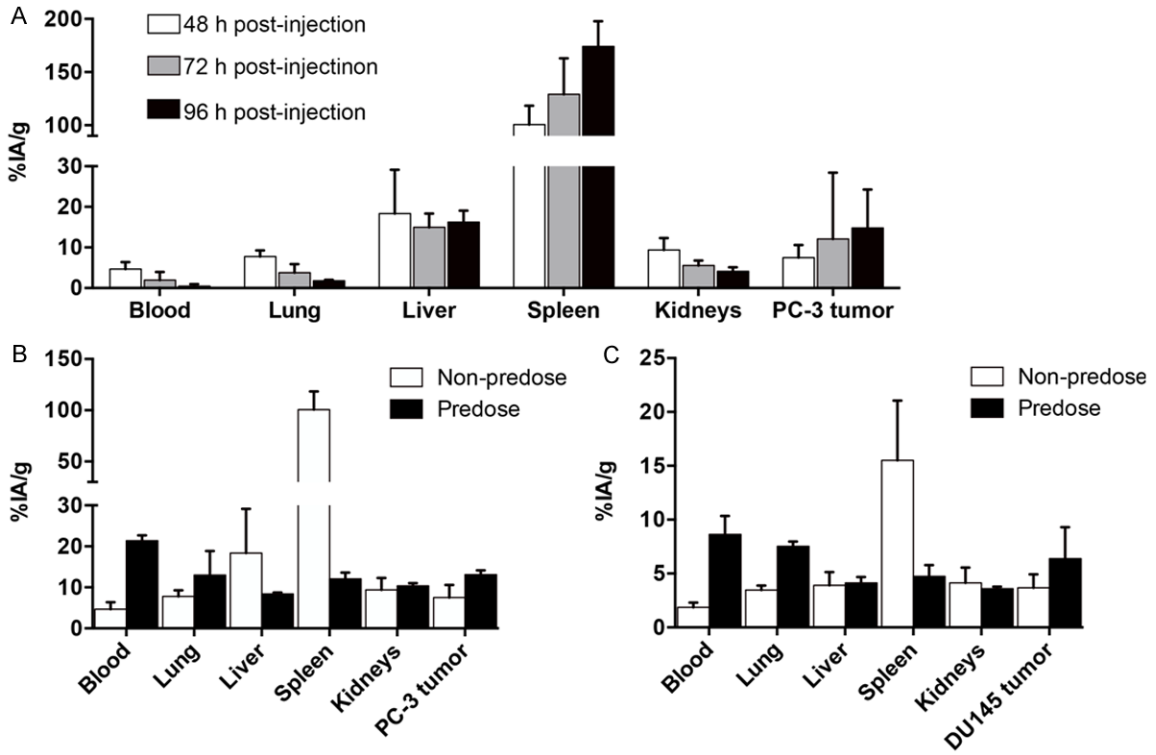

Figure 3. *Ex vivo* biodistribution data of ^{111}In-DTPA-INCA-X. The percent of injected activity per gram of tissue (%IA/g) of ^{111}In-DTPA-INCA-X (0.3-0.4 MBq, 20 μg of INCA-X). (A) 48 hours (white bars), 72 hours (light gray bars) and 96 hours (black bars) post-injection in nude mice bearing PC-3 xenografts and (B) 48 hours post-injection in nude mice bearing PC-3 xenografts (white bars). One group of mice received a predose of cold DTPA-INCA-X (1 mg) 24 hours prior to ^{111}In-DTPA-INCA-X (0.3-0.4 MBq [8-11 μCi], 15 μg of INCA-X) (black bars). (C) Uptake of ^{111}In-DTPA-INCA-X 48 hours post-injection in nude mice bearing DU145 xenografts (white bars). One group of mice received a predose of cold DTPA-INCA-X (1.6 mg) 24 hours prior to ^{111}In-DTPA-INCA-X (same amount as (B); black bars). Error bars represent mean ± SD.

Figure 2B. The internalization rate of ^{111}In-DTPA-INCA-X in PC-3 cells increased over time and had internalized by approximately 40% by 72 hours after interrupted incubation. The retention of the conjugate displayed the same pattern and seemed to continue to increase after 72 hours when the assay was stopped.

Biodistribution and preclinical SPECT/CT imaging of ^{111}In-DTPA-INCA-X in PC-3 and PC-3M-Lu2 tumor-bearing mice

The ^{111}In-DTPA-INCA-X antibody biodistribution in the major organs, blood and tumors of mice bearing subcutaneous PC-3 tumors was ascertained from the %IA/g values (**Table 1** and **Figure 3A**). The biodistribution in non-predosed mice revealed the majority of activity in the spleen (consistent with SPECT images of PC-3M-Lu2 xenografted mice; **Figure 4**), followed by the liver, tumor and kidneys. Low to moderate uptake in other organs was also noted. Antibody localization to the tumor nearly doubled from approximately 8 %IA/g (SD 3) at 48 hours to 15 %IA/g (SD 9) at 96 hours post-injection of ^{111}In-DTPA-INCA-X (**Table 1**). The mean uptake values presented in **Table 1** also show localization to the spleen, which increased over time from the first measurement of 101 %IA/g (SD 18) at 48 hours to 174 %IA/g (SD 23) at 96 hours post-injection. There was a marked decrease of activity from all other tissues and blood with time, showing the antibody is not retained in non-specific organs (**Table 1**). Notably, the organ-to-blood ratios in **Table 2** increased over time in the major organs and tumor, indicating there was an active uptake. But, as illustrated in **Table 3**, the tumor-to-organ ratios also increased over time in all organs, except in the spleen, thus confirming tumor specificity. Despite the high uptake in the spleen of non-predosed mice, ^{111}In-DTPA-

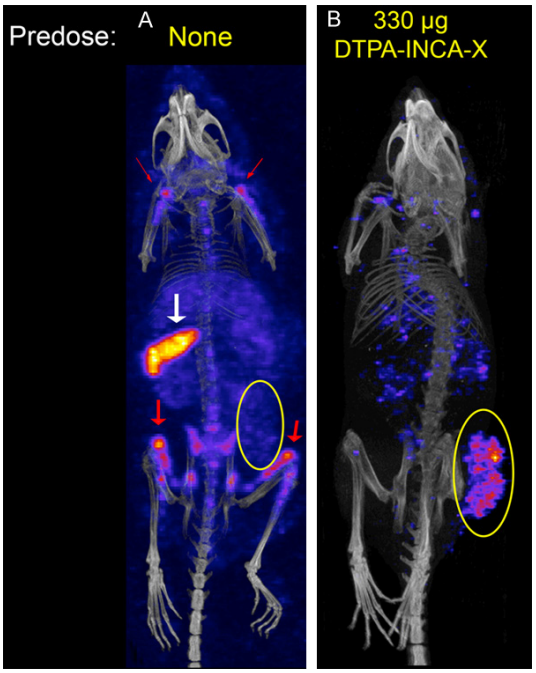

Figure 4. SPECT/CT images of nude mice bearing PC-3M-Lu2 xenografts. Posterior projections of mice injected with (A) ^{111}In-DTPA-INCA-X (10-15 MBq (270-405 µCi), 20 µg INCA-X) and (B) pre-administered intravenously cold DTPA-INCA-X (approx. 330 µg) followed one day later by ^{111}In-DTPA-INCA-X (same amount as in (A)). The mice were imaged 48 hours post-injection of ^{111}In-DTPA-INCA-X. Tumors are circled in yellow, white arrow points to spleen and red arrows indicate activity in red bone marrow.

INCA-X accumulated well in tumors, with a tumor-to-blood ratio around 30 by 96 hours post-injection (**Table 3**).

Interestingly, mice pre-administered with cold DTPA-INCA-X displayed significantly higher accumulation of activity in the tumors (P = 0.03) increasing from 8 %IA/g (SD 3) to 13 %IA/g (SD 1) (**Table 1** and **Figure 5A**), and significantly reduced activity in the spleen (P = 0.002) from 101 %IA/g (SD 18) to 12 %IA/g (SD 2) (**Table 1** and **Figure 5B**) at 48 hours post-injection of ^{111}In-DTPA-INCA-X. The tumor-to-organ uptake ratios of mice pre-administered cold DTPA-INCA-X were improved in comparison with the mice that only received ^{111}In-DTPA-INCA-X (**Table 3**), yet the blood concentration increased (**Table 1** and **Figure 3B**). The SPECT/CT images of mice with and without a predose of DTPA-INCA-X (**Figure 4**) effectively mirror the *ex vivo* biodistribution results (**Table 1**). The image of the non-predosed mouse shown in **Figure 4** reveals the majority of activity is in the

Table 2. Organ-to-blood ratios in nude mice bearing PC-3 tumors

	48 h (predose, n = 3)	48 h (n = 4)	72 h (n = 4)	96 h (n = 4)
Tumor	0.61	1.61	6.07	30.22
Spleen	0.56	21.67	64.82	355
Lungs	0.61	1.67	1.89	3.71
Kidneys	0.49	2.02	2.81	8.43
Liver	0.39	3.94	7.53	33.10
Prostate	0.61	1.78	2.73	14.09
Muscle	0.15	0.16	0.27	1.35
Brain	0.03	0.35	0.74	1.22

Table 3. Tumor-to-organ ratios in nude mice bearing PC-3 tumors

	48 h (predose, n = 3)	48 h (n = 4)	72 h (n = 4)	96 h (n = 4)
Spleen	1.09	0.07	0.09	0.09
Lungs	1.01	0.96	3.20	8.14
Kidneys	1.26	0.80	2.16	3.59
Liver	1.55	0.41	0.81	0.91
Prostate	1.01	0.91	2.22	2.15
Muscle	4.02	10.29	22.37	22.44
Brain	19.33	4.67	8.15	24.76
Blood	0.61	1.61	6.07	30.22

spleen (white arrow) with fairly homogenous, low activity in the major blood rich organs and slightly higher uptake in the red bone marrow (red arrows). Conversely, the SPECT/CT images also show that by pre-administering a dose of cold DTPA-INCA-X 24 hours prior to the labeled antibody, we could significantly boost the accumulation of ^{111}In-DTPA-INCA-X in the tumors (tumor circled in yellow).

Our *in vivo* and *ex vivo* tests confirmed that by pre-administering non-labeled, DTPA-conjugated INCA-X before intravenous injection of the labeled antibody, we were able to significantly reduce the off-target binding of the labeled antibody and increase the tumor targeting capability of ^{111}In-DTPA-INCA-X to PC-3 and PC-3M-Lu2 human xenografts in nude mice.

Biodistribution and preclinical SPECT/CT imaging of ^{111}In-DTPA-INCA-X in DU145 tumor-bearing mice

The biodistribution results of ^{111}In-DTPA-INCA-X, as determined from %IA/g in various organs

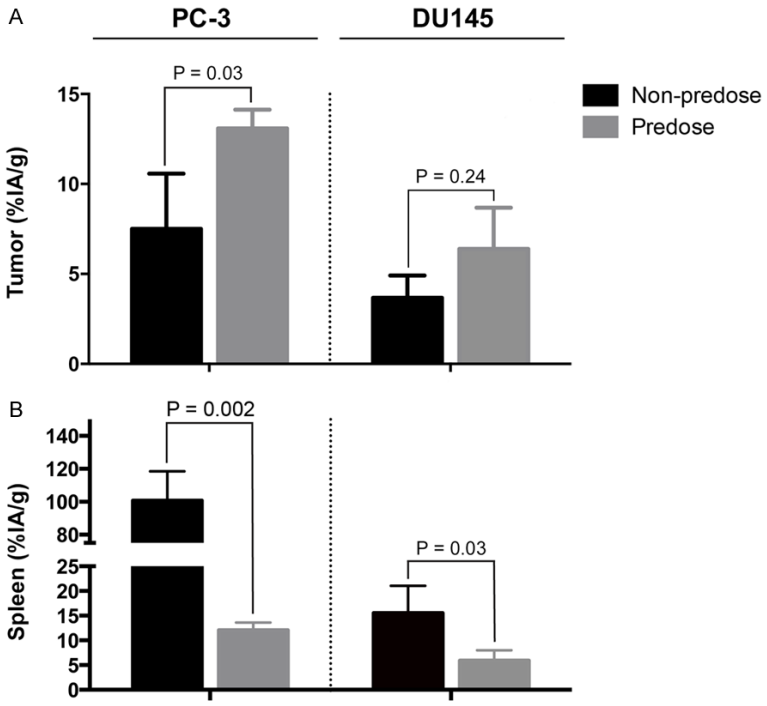

Figure 5. *In vivo* comparison of ^{111}In-DTPA-INCA-X uptake in the tumors and spleens of nude mice bearing PC-3 or DU145 xenograft tumors. The uptake results are presented as %IA/g in (A) the tumors and (B) the spleens. Predosed mice were administered 1 mg (PC-3) or 1.6 mg (DU145) non-labeled DTPA-INCA-X one day before ^{111}In-DTPA-INCA-X (0.3-0.4 MBq [8-11 μCi], 15-20 μg of INCA-X). Black bars represent non-predosed and gray bars represent predosed mice. Error bars represent mean ± SD.

and tumor of nude mice bearing DU145 tumors (**Figure 3C**), show strong similarities to the results of nude mice bearing PC-3 tumors (**Figure 3B**). Similar to our findings in non-predosed mice bearing PC-3 tumors, the majority of activity in mice bearing human DU145 xenografts was also concentrated to the spleen at 48 hours post-injection of ^{111}In-DTPA-INCA-X (16 %IA/g (SD 6)). Low to marginal uptake values were noted in the kidney (4 %IA/g (SD 1)), liver (4 %IA/g (SD 1)), lungs (3.47 %IA/g (SD 0.41)) and blood pool (1.87 %IA/g (SD 0.44)) (**Figure 3C**). Moreover, by intravenously pre-administering cold DTPA-INCA-X 24 hours prior to ^{111}In-DTPA-INCA-X, we were able to block the off target uptake and 'redirect' the antibody to the tumors (**Figures 3C** and **5**).

The SPECT/CT images of DU145 tumor-bearing mice were consistent with the *ex vivo* biodistribution data in regards to predose group 1 versus non-predosed animals. Namely, the majority of activity was concentrated to the spleen of non-predosed animals (**Figure 6A**, white arrow) 48 hours post-injection of the labeled antibody. The image of predose group 1 animal, which was pre-administered cold DTPA-INCA-X 24 hours prior to administering ^{111}In-DTPA-INCA-X, showed increased localization to the tumor (**Figure 6C**, circled in yellow); however, there was background activity from circulating antibody in highly vascularized organs and blood. For that reason, we conducted an additional study to determine whether administering the predose of cold antibody at different time-points would affect the outcome. Therefore, mice bearing DU145 xenografts were pre-administered cold DTPA-INCA-X 48 hours (predose group 2; **Figure 6D**) or directly before (predose group 3; **Figure 6B**) the radiolabeled antibody was intravenously administered. The animals were imaged with the SPECT/CT camera 48 hours after ^{111}In-DTPA-INCA-X administration. The images with the highest tumor uptake were collected from mice pre-administered DTPA-INCA-X 48 hours prior to the labeled INCA-X (predose group 2; **Figure 6D**). Mice predosed directly before ^{111}In-DTPA-INCA-X was administered (predose group 3; **Figure 6B**), had less circulating activity than observed in predose group 1 animals (**Figure 6C**), but still more than observed in the predose group 2 animals (**Figure 6D**). Yet, regardless of when the predose was administered, the spleen of all animals pre-administered cold DTPA-INCA-X was effectively blocked and there was an obvious increased accumulation of ^{111}In-DTPA-INCA-X in all of the tumors (**Figures 5** and **6**, tumors circled in yellow).

Discussion

INCA-X is a human antibody originally selected from a large naïve antibody library, using selective tumor up regulated antigens and internalization as selection and screening criteria. In this paper we confirmed INCA-X binding to the surface of viable PC-3 cells (**Figure 1**). The pres-

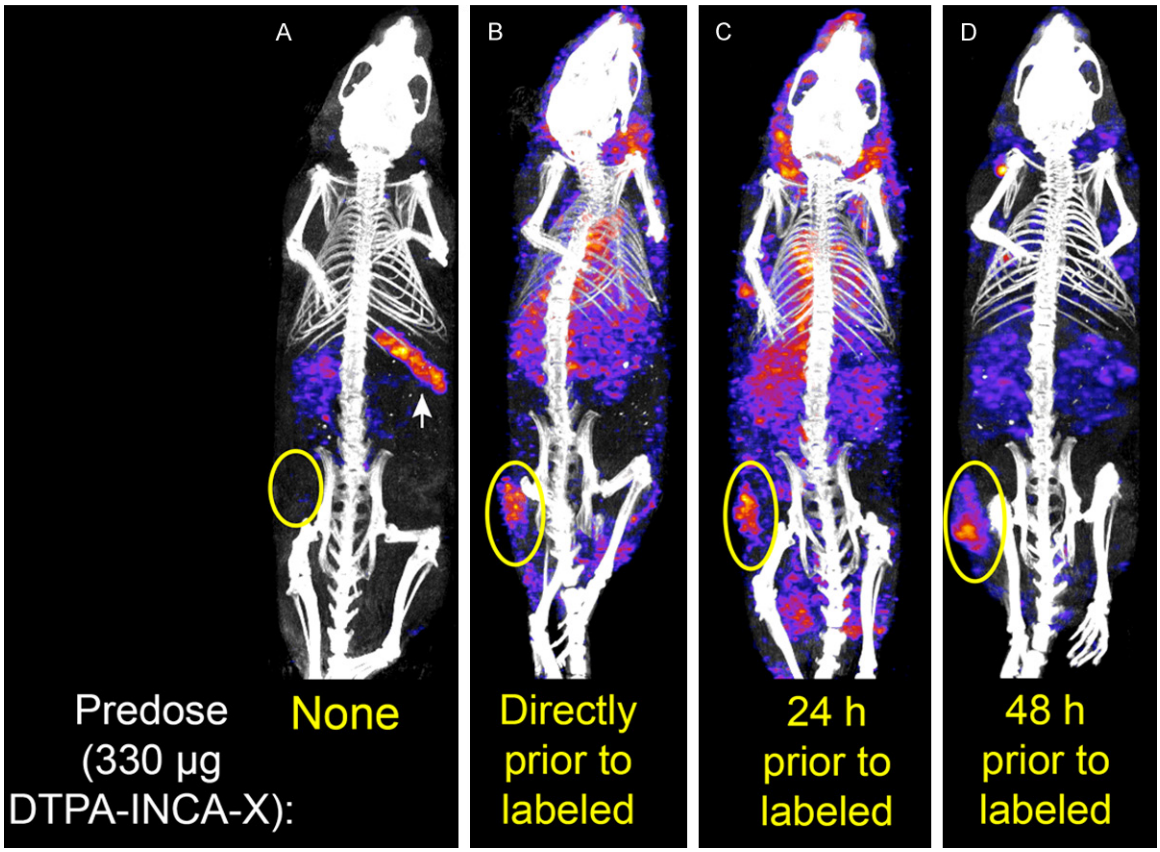

Figure 6. SPECT/CT images of nude mice bearing DU145 xenograft tumors. Anterior projections of mice injected with (A) only ^{111}In-DTPA-INCA-X (10-15 MBq (270-405 µCi), 20 µg INCA-X) and pre-administered (B) cold DTPA-INCA-X (approx. 330 µg) immediately followed by ^{111}In-DTPA-INCA-X (same amount as in (A)), (C) cold DTPA-INCA-X followed one day later by ^{111}In-DTPA-INCA-X (same amounts as in (A)) and (D) cold DTPA-INCA-X followed two days later by ^{111}In-DTPA-INCA-X (same amounts as in (A)). All mice were imaged 48 hours post-injection of ^{111}In-DTPA-INCA-X. Tumors are circled in yellow and white arrow points to the spleen.

ence of the proteins was documented through specific anti-peptide antibodies, anti-Ku70 (amino acids 506-541) and anti-Ku80 (amino acids 610-705). The Ku70 and Ku80 proteins are known to take part in a plethora of essential functions in the eukaryotic cell, with their chaperon function in the Ku-dependent NHEJ repair pathway of DSB as the most documented feature [19, 29]. One hallmark of tumors is genomic instability often manifested as DSB. DNA double strand breaks are induced by several different endogenous and exogenous factors and thus mammalian cells have developed a number of repair systems to meet the challenge of DNA damage, of which the Ku70/Ku80 associated NHEJ pathway is very important. Ku70/Ku80 proteins are generally associated with the nucleus, yet are frequently found in cytoplasm and on the cell surface. In non-malignant cells, Ku70 is also reported to have a function at the cell surface and acts as a receptor for *Rickettsia conori* uptake into non-phagocytic mammalian cells [30, 31] or as a receptor for DNA [13].

The aim of this study was to make a first evaluation of the Ku70/Ku80 *in vivo* availability, up regulation and essential function as a target candidate for antibody imaging. Using ^{111}In labeled, DTPA-conjugated INCA-X antibody, we confirmed the binding and internalization of the antibody on PC-3 cells (**Figure 2**), previously reported with ^{125}I labeled antibody on PL45 pancreatic cell line [7]. When injected into animals with xenografts of human prostate cancer cell lines known to express the target antigen *in vivo*, a significant tumor uptake could be seen with SPECT/CT imaging only after pre-administering non-labeled antibody (**Figures 4** and **6B-D**). This finding differed from our *in vitro*

blocking tests on the PC-3 cell line where the ^{111}In-DTPA-INCA-X uptake on PC-3 cells was significantly blocked with a predose of cold INCA-X (**Figure 2A**). Specific accumulation of ^{111}In-DTPA-INCA-X in the human prostate cancer-based xenografts was observed after the pre-administration of cold DTPA-INCA-X, whereas uptake in other organs was negligible and eliminated with time, except for the spleen. In animals pre-administered DTPA-INCA-X, there was a shift of activity from the spleen to the blood pool and tumor (**Figure 3B** and **3C**), indicating a block of a dominating off target effect. The shift of activity indicates that ^{111}In-DTPA-INCA-X antibody is capable of targeting human prostate cancer-based xenografts in mice that first receive a predose of cold antibody. Some antigen in the spleen appears to be rapidly targeted but also easily blocked with a suitable pre-administered dose of DTPA-conjugated, non-labeled antibody. The nature of this binding is preliminary interpreted as an off target binding (cross reactivity) rather than an indication of the expression of available Ku70/Ku80 antigen on murine cells. Using immune precipitation with INCA-X attached to magnetic beads via Protein G and extracts of 1% NP 40 solubilized tissue, INCA-X could be shown to readily precipitate Ku70/Ku80 complex from all human cell lines tested [7] but not from any mouse tumor cell line or from solubilized mouse spleen. These results indicate that the antibody does not bind the mouse Ku70/Ku80 complex and thus the localization seen with the labeled DTPA-INCA-X is the result of a low avidity binding to another epitope.

The biodistribution data of mice bearing PC-3 xenografts (**Table 1**) showed the uptake of labeled antibody in the spleen and tumor were both increased with time post-injection of ^{111}In-DTPA-INCA-X and reached a maximum after 96 hours when the study was ended. The differences in the biodistribution and SPECT images between the more aggressive PC-3/PC-3M-Lu2 tumor-bearing mice and the DU145 tumor-bearing mice, with regards to the significant level of activity redirected to the tumors and the clarity of predose group 1 SPECT images, could be due to differences in the expression of the Ku70/Ku80 antigen on the surface of the cells. The Ku70/Ku80 expression on both cell lines is thought to be similar [27], yet it is feasible that the more aggressive cells have a higher cell surface expression than that on the less aggressive cell lines.

Various biomarkers have been mentioned as imaging and therapeutic candidates. PSMA is a clinically valid tumor biomarker for prostate cancer; however, its true impact in the clinical setting has not been made apparent. ProstaScint® is currently the only clinically approved radiolabeled antibody for imaging prostate cancer, yet one of the downfalls of ProstaScint® is that it targets the internal domain of PSMA making image interpretation complex and thus results in a high number of false positives and false negatives [32, 33]. There is now more focus on targeting the external domain of PSMA, which shows promise [34]. Obviously there is room for new approaches, and at least four antibody-drug conjugates targeting prostate cancer are in the early stage of clinical development: anti-PSMA from Progenics Pharmaceuticals, Inc. (http://clinicaltrials.gov NLM identifier: NCT01414283), anti-secondary lymphoid tissue chemokine, SLC-44A2, (ASG-5ME) and anti-prostate stem cell antigen monoclonal antibody, AGS-1C4D4, from Astellas Pharma (http://clinicaltrials.gov NLM identifiers: NCT01228760 and NCT00-519233, respectively) and anti-TROP2 (IMMU-132) from Immunomedics, Inc. (http://clinicaltrials.gov NLM identifier: NCT01631552).

The INCA-X antibody was selected and screened for its capacity to internalize into several different carcinoma cell lines, defining a rapidly internalizing structure up regulated on a majority of cancer cell lines and possibly down regulated after castration therapy. This antibody has the capacity to deliver toxins or radionuclides to tumors *in vitro* and localize to tumors *in vivo*, particularly if the off target binding is minimized with a predose of cold antibody. Moreover, if the expression of the Ku proteins is down regulated after castration therapy, it could be possible to assess the surface expression and estimate the optimal time for starting curative radiotherapy by determining when the patient is the most radiosensitive. The biodistribution and SPECT images of all PC-3, PC-3M-Lu2 and DU145 tumor-bearing mice, pre-administered cold DTPA-INCA-X, showed strong localization of radioactivity in the tumors (**Figures 4**, **5A** and **6B-D**) and significantly lower uptake in the spleens (**Figure 5B**) and other major organs (**Table 1** and **Figure 3B**, **3C**). Based on our find-

ings, we believe that the INCA-X antibody defines a target worth further evaluation. As this was the first study assessing the INCA-X antibody in a living system, the difference between uptake of labeled antibody with and without a pre-administered dose of DTPA-INCA-X in human prostate cancer cell lines and in nude mice bearing human prostate cancer-based xenografts needs to be further investigated. Nevertheless, the results are encouraging to go further and try to improve the tumor uptake by testing newly generated antibodies directed to the Ku70/Ku80 antigen.

Conclusion

The ^{111}In-DTPA-INCA-X antibody can target and internalize into subcutaneous xenografts of prostate cancer cell lines in mice pre-administrated non-labeled, DTPA-conjugated INCA-X antibody, thus identifying the Ku70/Ku80 antigens as targets worth further investigation.

Acknowledgements

We wish to thank Nina Persson (BioInvent Int. AB, Lund, Sweden) and Ms. Elise Nilsson at the Department of Laboratory Medicine, Center for Molecular Pathology in Malmö, Lund University, Sweden for their excellent technical assistance. We would also like to thank Mrs. Jennifer Corley for her proofing and suggestions. Lund University Bioimaging Center is gratefully acknowledged for providing experimental resources. The authors also want to acknowledge: Swedish Cancer Foundation, Mrs. Berta Kamprad Foundation, Gunnar Nilsson Cancer Foundation, Government Funding of Clinical Research within the National Health Services, Lund University (ALF) and IngaBritt and Arne Lundberg Foundation for their financial support.

Disclosure of conflict of interest

The authors have no affiliations, memberships, funding, or financial holdings that might be perceived as affecting the objectivity of this publication.

Address correspondence to: Susan Evans-Axelsson, Division of Urological Cancers, Department of Clinical Sciences, Lund University, Skåne University Hospital Malmö, Jan Waldenströms gatan 59, SE205 02 Malmö, Sweden. E-mail: Susan.evans-axelsson@med.lu.se

References

[1] Luo J, Duggan DJ, Chen Y, Sauvageot J, Ewing CM, Bittner ML, Trent JM and Isaacs WB. Human prostate cancer and benign prostatic hyperplasia: molecular dissection by gene expression profiling. Cancer Res 2001; 61: 4683-4688.

[2] Schubert M, Spahn M, Kneitz S, Scholz CJ, Joniau S, Stroebel P, Riedmiller H and Kneitz B. Distinct microRNA expression profile in prostate cancer patients with early clinical failure and the impact of let-7 as prognostic marker in high-risk prostate cancer. PLoS One 2013; 8: e65064.

[3] Taylor BS, Schultz N, Hieronymus H, Gopalan A, Xiao Y, Carver BS, Arora VK, Kaushik P, Cerami E, Reva B, Antipin Y, Mitsiades N, Landers T, Dolgalev I, Major JE, Wilson M, Socci ND, Lash AE, Heguy A, Eastham JA, Scher HI, Reuter VE, Scardino PT, Sander C, Sawyers CL and Gerald WL. Integrative genomic profiling of human prostate cancer. Cancer Cell 2010; 18: 11-22.

[4] Beresford MJ, Gillatt D, Benson RJ and Ajithkumar T. A systematic review of the role of imaging before salvage radiotherapy for post-prostatectomy biochemical recurrence. Clin Oncol (R Coll Radiol) 2010; 22: 46-55.

[5] Knowles SM and Wu AM. Advances in immuno-positron emission tomography: antibodies for molecular imaging in oncology. J Clin Oncol 2012; 30: 3884-3892.

[6] Soderlind E, Strandberg L, Jirholt P, Kobayashi N, Alexeiva V, Aberg AM, Nilsson A, Jansson B, Ohlin M, Wingren C, Danielsson L, Carlsson R and Borrebaeck CA. Recombining germline-derived CDR sequences for creating diverse single-framework antibody libraries. Nat Biotechnol 2000; 18: 852-856.

[7] Fransson J and Borrebaeck CA. The nuclear DNA repair protein Ku70/80 is a tumor-associated antigen displaying rapid receptor mediated endocytosis. Int J Cancer 2006; 119: 2492-2496.

[8] Mimori T, Akizuki M, Yamagata H, Inada S, Yoshida S and Homma M. Characterization of a high molecular weight acidic nuclear protein recognized by autoantibodies in sera from patients with polymyositis-scleroderma overlap. J Clin Invest 1981; 68: 611-620.

[9] Mimori T, Hardin JA and Steitz JA. Characterization of the DNA-binding protein antigen Ku recognized by autoantibodies from patients with rheumatic disorders. J Biol Chem 1986; 261: 2274-2278.

[10] Ponnala S, Veeravalli KK, Chetty C, Dinh DH and Rao JS. Regulation of DNA repair mechanism in human glioma xenograft cells both in vitro and in vivo in nude mice. PLoS One 2011; 6: e26191.

[11] Koike M, Yutoku Y and Koike A. KARP-1 works as a heterodimer with Ku70, but the function of KARP-1 cannot perfectly replace that of Ku80 in DSB repair. Exp Cell Res 2011; 317: 2267-2275.
[12] Koike M. Dimerization, translocation and localization of Ku70 and Ku80 proteins. J Radiat Res (Tokyo) 2002; 43: 223-236.
[13] Al-Ubaidi FL, Schultz N, Loseva O, Egevad L, Granfors T and Helleday T. Castration therapy results in decreased Ku70 levels in prostate cancer. Clin Cancer Res 2013; 19: 1547-1556.
[14] Taccioli GE, Gottlieb TM, Blunt T, Priestley A, Demengeot J, Mizuta R, Lehmann AR, Alt FW, Jackson SP and Jeggo PA. Ku80: product of the XRCC5 gene and its role in DNA repair and V(D)J recombination. Science 1994; 265: 1442-1445.
[15] d'Adda di Fagagna F, Hande MP, Tong WM, Roth D, Lansdorp PM, Wang ZQ and Jackson SP. Effects of DNA nonhomologous end-joining factors on telomere length and chromosomal stability in mammalian cells. Curr Biol 2001; 11: 1192-1196.
[16] Featherstone C and Jackson SP. Ku, a DNA repair protein with multiple cellular functions? Mutat Res 1999; 434: 3-15.
[17] Hsu HL, Gilley D, Blackburn EH and Chen DJ. Ku is associated with the telomere in mammals. Proc Natl Acad Sci U S A 1999; 96: 12454-12458.
[18] Woodard RL, Lee KJ, Huang J and Dynan WS. Distinct roles for Ku protein in transcriptional reinitiation and DNA repair. J Biol Chem 2001; 276: 15423-15433.
[19] Mayeur GL, Kung WJ, Martinez A, Izumiya C, Chen DJ and Kung HJ. Ku is a novel transcriptional recycling coactivator of the androgen receptor in prostate cancer cells. J Biol Chem 2005; 280: 10827-10833.
[20] Muller C, Paupert J, Monferran S and Salles B. The double life of the Ku protein: facing the DNA breaks and the extracellular environment. Cell Cycle 2005; 4: 438-441.
[21] Cherepanova AV, Bushuev AV, Duzhak TG, Zaporozhchenko IA, Vlassov VV and Laktionov PP. Ku protein as the main cellular target of cell-surface-bound circulating DNA. Expert Opin Biol Ther 2012; 12 Suppl 1: S35-41.
[22] Monferran S, Muller C, Mourey L, Frit P and Salles B. The Membrane-associated form of the DNA repair protein Ku is involved in cell adhesion to fibronectin. J Mol Biol 2004; 337: 503-511.
[23] Persson O, Salford LG, Fransson J, Widegren B, Borrebaeck CA and Holmqvist B. Distribution, cellular localization, and therapeutic potential of the tumor-associated antigen Ku70/80 in glioblastoma multiforme. J Neurooncol 2010; 97: 207-215.
[24] Prabhakar BS, Allaway GP, Srinivasappa J and Notkins AL. Cell surface expression of the 70-kD component of Ku, a DNA-binding nuclear autoantigen. J Clin Invest 1990; 86: 1301-1305.
[25] Dalziel RG, Mendelson SC and Quinn JP. The nuclear autoimmune antigen Ku is also present on the cell surface. Autoimmunity 1992; 13: 265-267.
[26] Junutula JR, Raab H, Clark S, Bhakta S, Leipold DD, Weir S, Chen Y, Simpson M, Tsai SP, Dennis MS, Lu Y, Meng YG, Ng C, Yang J, Lee CC, Duenas E, Gorrell J, Katta V, Kim A, McDorman K, Flagella K, Venook R, Ross S, Spencer SD, Lee Wong W, Lowman HB, Vandlen R, Sliwkowski MX, Scheller RH, Polakis P and Mallet W. Site-specific conjugation of a cytotoxic drug to an antibody improves the therapeutic index. Nat Biotechnol 2008; 26: 925-932.
[27] Chen CS, Wang YC, Yang HC, Huang PH, Kulp SK, Yang CC, Lu YS, Matsuyama S and Chen CY. Histone deacetylase inhibitors sensitize prostate cancer cells to agents that produce DNA double-strand breaks by targeting Ku70 acetylation. Cancer Res 2007; 67: 5318-5327.
[28] Norderhaug L, Olafsen T, Michaelsen TE and Sandlie I. Versatile vectors for transient and stable expression of recombinant antibody molecules in mammalian cells. J Immunol Methods 1997; 204: 77-87.
[29] Parvathaneni S, Stortchevoi A, Sommers JA, Brosh RM Jr and Sharma S. Human RECQ1 interacts with Ku70/80 and modulates DNA end-joining of double-strand breaks. PLoS One 2013; 8: e62481.
[30] Chan YG, Cardwell MM, Hermanas TM, Uchiyama T and Martinez JJ. Rickettsial outer-membrane protein B (rOmpB) mediates bacterial invasion through Ku70 in an actin, c-Cbl, clathrin and caveolin 2-dependent manner. Cell Microbiol 2009; 11: 629-644.
[31] Martinez JJ, Seveau S, Veiga E, Matsuyama S and Cossart P. Ku70, a component of DNA-dependent protein kinase, is a mammalian receptor for Rickettsia conorii. Cell 2005; 123: 1013-1023.
[32] Tsivian M, Wright T, Price M, Mouraviev V, Madden JF, Kimura M, Wong T and Polascik TJ. 111-In-capromab pendetide imaging using hybrid-gamma camera-computer tomography technology is not reliable in detecting seminal vesicle invasion in patients with prostate cancer. Urol Oncol 2012; 30: 150-154.
[33] Haseman MK, Rosenthal SA and Polascik TJ. Capromab Pendetide imaging of prostate cancer. Cancer Biother Radiopharm 2000; 15: 131-140.
[34] Tagawa ST, Milowsky MI, Morris M, Vallabhajosula S, Christos P, Akhtar NH, Osborne J,

Goldsmith SJ, Larson S, Taskar NP, Scher HI, Bander NH and Nanus DM. Phase II study of Lutetium-177-labeled anti-prostate-specific membrane antigen monoclonal antibody J591 for metastatic castration-resistant prostate cancer. Clin Cancer Res 2013; 19: 5182-5191.